

Opposing Effects of Reflective and Nonreflective Planetary Wave Breaking on the NAO

JOHN T. ABATZOGLOU AND GUDRUN MAGNUSDOTTIR

Department of Earth System Science, University of California, Irvine, Irvine, California

(Manuscript received 16 September 2005, in final form 4 April 2006)

ABSTRACT

Planetary wave breaking (PWB) over the subtropical North Atlantic is observed over 45 winters (December 1958–March 2003) using NCEP–NCAR reanalysis data. PWB is manifested in the rapid, large-scale and irreversible overturning of potential vorticity (PV) contours on isentropic surfaces in the subtropical upper troposphere. As breaking occurs over the subtropical North Atlantic, an upper-tropospheric PV tripole anomaly forms with nodes over the subtropical, midlatitude, and subpolar North Atlantic. The northern two nodes of this tripole are quite similar to the spatial structure of the North Atlantic Oscillation (NAO), with positive polarity.

Nonlinear reflection is identified in approximately a quarter of all PWB events. Following breaking, two distinct circulation regimes arise, one in response to reflective events and the other in response to nonreflective events. For reflective events, anomalies over the North Atlantic rapidly propagate away from the breaking region along a poleward arching wave train over the Eurasian continent. The quasi-stationary wave activity flux indicates that wave activity is exported out of the Atlantic basin. At the same time, the regional poleward eddy momentum flux goes through a sign reversal, as does the polarity of the NAO. For nonreflective events, the dipole anomaly over the North Atlantic amplifies. Diagnostics for nonreflective events suggest that wave activity over the Azores gets absorbed, allowing continued enhancement of both the regional poleward eddy momentum flux and the positive NAO.

1. Introduction

Quasi-stationary planetary waves, as other Rossby waves, depend on a background potential vorticity (PV) gradient for their restoring mechanism. Observational studies (e.g., Wallace and Hsu 1983) have shown that tropospheric low-frequency disturbances tend to be longitudinally localized wave trains traveling along great circle routes, rather than being “monochromatic” waves with a well-defined longitudinal wavenumber. As a wave train propagates to lower latitudes, where the westerly background flow is weak, it amplifies and its phase lines acquire a positive tilt (NE–SW), associated with a poleward momentum flux. A small-amplitude wave train may be “absorbed” close to its critical latitude, the latitude at which the phase speed of the wave matches the background flow. This means

that the wave train weakens and disappears (due to diabatic effects) without mixing up the PV field and affecting the large-scale flow. However, if the wave amplitude is large enough, the wave may break, resulting in the mixing of PV over a finite region. Planetary wave breaking (PWB) is manifested by the large-scale and rapid, irreversible overturning of PV contours on isentropic surfaces (McIntyre and Palmer 1983).

Figure 1 shows an example of a PWB event over the North Atlantic on 4 February 1996. This event is typical of wintertime anticyclonic (on the anticyclonic or equatorward side of the jet) PWB over the North Atlantic. Wave trains typically propagate along the strong PV gradient over the North American continent. This gradient inhibits meridional wave excursions and allows for the formation of a waveguide. A weaker PV gradient over the mid-Atlantic, near the jet exit region, allows waves to propagate equatorward (Fig. 1a). As a wave train approaches the weak background flow over the subtropical Atlantic, it amplifies and imposes a strong poleward eddy momentum flux. The breaking event is clearly noted by observing the dramatic over-

Corresponding author address: Prof. Gudrun Magnusdottir, Dept. of Earth System Science, University of California, Irvine, Irvine, CA 92697-3100.
E-mail: gudrun@uci.edu

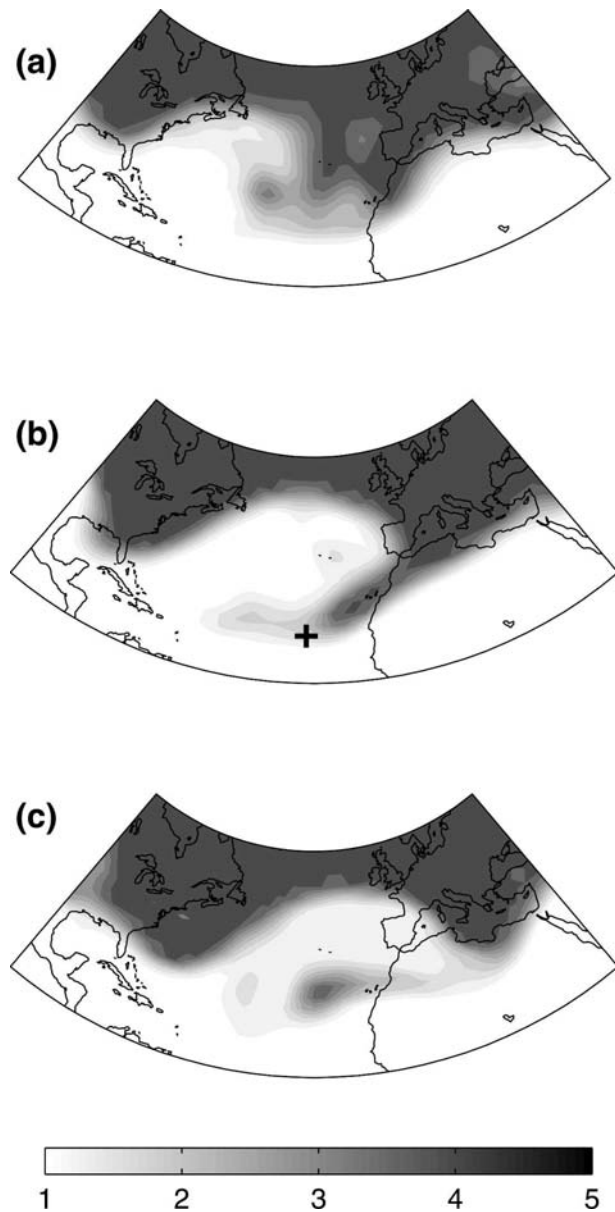


FIG. 1. A PWB event occurring on 4 Feb 1996. The PV (in PVU) on the 340-K isentropic surface is shown (a) 2 days prior, (b) on the day of, and (c) 2 days after PWB. The spot where breaking is first detected (according to the criteria in section 2) is indicated by a heavy plus sign in (b).

turning of PV contours about the isoline of 2 PVU (which approximates the tropopause; $1 \text{ PVU} = 10^{-6} \text{ K m}^2 \text{ s}^{-1} \text{ kg}^{-1}$) in Fig. 1b. Following the breaking, rapid large-scale advective mixing ensues (Fig. 1c).

PWB can impact the large-scale atmospheric circulation both in the Tropics and extratropics. The influx of high-PV air into the Tropics as a result of breaking can induce large-scale tropical convection (Kiladis 1998). PWB also contributes to stratosphere–troposphere ex-

change along isentropic surfaces across the subtropical tropopause (Holton et al. 1995). A hierarchy of modeling studies have shown that PWB may result in nonlinear reflection (or reradiation) of planetary waves into midlatitudes (Brunet and Haynes 1996; Magnusdottir and Haynes 1999; Magnusdottir and Walker 2000; Walker and Magnusdottir 2002, 2003). Nonlinear reflection can profoundly influence the extratropical flow field by altering stationary waves and associated teleconnection patterns. Abatzoglou and Magnusdottir (2004) found evidence of nonlinear reflection following PWB in reanalysis datasets.

Upper-tropospheric, anticyclonic PWB is most frequently observed in summer over the western North Pacific and North Atlantic Basins. However, a localized region of frequent PWB (a so-called surf zone) can be found throughout the year over both basins. A majority of PWB events that occur in spring, summer, and fall are observed over the subtropical Pacific; however, in winter the vast majority of breaking events are observed over the central and eastern subtropical Atlantic (Abatzoglou and Magnusdottir 2006). The separation of the eddy-driven and subtropical jets over the Atlantic results in a much weaker subtropical zonal flow than over the Pacific. The weaker subtropical flow and weaker latitudinal PV gradient over the Atlantic basin weakens the quasi-stationary waveguide and increases the likelihood of PWB. The increased separation between the jets during winters that are characterized by the positive phase of the North Atlantic Oscillation (NAO) further augments PWB frequency. Abatzoglou and Magnusdottir (2006) found that nearly twice as many breaking events are observed during NAO positive winters than during NAO negative winters.

The strong poleward eddy momentum flux associated with wintertime PWB over the Atlantic may in turn influence the most prominent mode of low-frequency variability over the North Atlantic in winter, the NAO. Benedict et al. (2004) investigated the synoptic characteristics of the intraseasonal NAO. They found evidence that the positive (negative) phase of the NAO results from remnants of anticyclonic (cyclonic) synoptic wave breaking.¹ Feldstein (2003) found that the life cycle of the (high frequency) NAO has a time scale of around 2 weeks and is driven primarily by the nonlinear eddy vorticity flux. These results are supported by simple dynamical modeling studies that find that the spatial and temporal characteristics of the in-

¹ Their life cycle of anticyclonic breaking is quite similar to the event shown in Fig. 1.

traseasonal NAO arise through variations in the momentum flux (e.g., Vallis et al. 2004).

In this paper we examine the effects of anticyclonic, wintertime PWB over the North Atlantic Basin on the extratropical atmospheric flow in National Centers for Environmental Prediction–National Center for Atmospheric Research (NCEP–NCAR) reanalysis data. We note strikingly different responses in the NAO life cycle following the breaking event, dependent on whether wave activity is absorbed locally or reflected poleward into midlatitudes. Section 2 describes the data and analysis methods used to objectively detect PWB and nonlinear reflection. Section 3 highlights the opposing impacts of reflective and nonreflective cases of PWB on the upper-tropospheric flow fields. The robust connection between PWB and both the intraseasonal and interannual NAO are discussed in section 4. Results are summarized and discussed in section 5.

2. Data and methodology

Daily mean upper-tropospheric flow fields over 45 winters (December 1958 to March 2003) from NCEP–NCAR reanalysis are used to detect PWB over the subtropical North Atlantic sector. PWB is identified by analyzing fields of PV in the upper troposphere/lower stratosphere. We calculate PV on three isentropic surfaces (350, 340, and 330 K) that span the subtropical tropopause over the Atlantic in winter (Abatzoglou and Magnusdottir 2006). By constraining our analysis of large-scale wave breaking to isentropic surfaces that intersect the subtropical tropopause and to latitudes between 10°–40°N, we are attempting to exclude baroclinic transients that typically break on lower isentropic surfaces and farther poleward from our wave breaking count. A PWB event is diagnosed upon first satisfying the following criteria involving the large-scale PV field:

- 1) There is a reversal in the latitudinal PV gradient about the tropopause such that a region of high PV ($PV > 2$ PVU) exists equatorward of a region of low PV ($PV < 1$ PVU).
- 2) There is a localized eastward PV gradient about the break, consistent with the notion of anticyclonic breaking.
- 3) The region of high (low) PV is part of a tongue of PV originating in the extratropics (Tropics).

The breaking point is defined as the southwesternmost point first satisfying the above criteria.

To ensure that only one event is counted per episode, all other PV reversals occurring within 4 days are discarded. Furthermore, when PWB is simultaneously

found on more than one vertical level, we only count the event on the highest isentropic surface.

Nonlinear reflection is diagnosed by using the latitudinal component of the 300-hPa stationary wave activity flux (Plumb 1985). PWB events where the initial, equatorward wave activity flux is followed by a reversed (i.e., poleward directed) flux following PWB, downstream and poleward of the wave-breaking region (Magnusdottir and Haynes 1999), are classified as reflective.

The wave activity flux is constructed from a 9-day time average, centered about the day of the breaking event. Reflection is noted if the area-averaged, wave activity flux is directed poleward over the region spanning 10°–20°N and 15°–60°E of the breaking point. The jet typically runs through this sector so that the wave activity flux is well defined. This region best captures the signal of reflection as seen in previous modeling studies (e.g., Walker and Magnusdottir 2003) as well as in observational studies (Abatzoglou and Magnusdottir 2004, 2006). This method of identifying nonlinear reflection is not sensitive to the exact number of days over which the flow field is averaged, as long as the chosen time frame includes the time period of reflection (i.e., 1–4 days after breaking).

Composites of both reflective and nonreflective events are formed by shifting analyzed fields in time with respect to the day of the initial PWB diagnosis. Note that since these composite fields are not shifted with respect to the exact location of the break (as was done in Abatzoglou and Magnusdottir 2006), we deemphasize the synoptic-scale features, and instead focus on the evolution of the large-scale patterns over the North Atlantic. Composites are formed from the 300-hPa wave activity flux, the 300-hPa eddy momentum flux, as well as anomalies in the 300-hPa streamfunction and PV on the 350-K surface (deviation from 45-yr daily mean; see next paragraph). The extratropical flow fields of interest show a near-equivalent barotropic structure with maximum amplitudes near the tropopause.

Anomalies are calculated with respect to each calendar day's time mean. The time means are computed by averaging the daily values for each calendar day over the entire 45-yr dataset, after which we apply a 20-day low-pass filter.

3. Results

A total of 576 PWB events are identified over the 45 winters. Most of these events are detected on the 330- and 340-K isentropic surfaces, coincident with the climatological three-dimensional structure of the winter



FIG. 2. Composite anomalous PV on the 350-K isentropic surface on the day of PWB. Contours exceeding the absolute value of 0.15 PVU are shown every 0.05 PVU.

subtropical tropopause over the North Atlantic (Abatzoglou and Magnusdottir 2006). The breaking event shown in Fig. 1 shows the typical anticyclonic meridional advection of low-PV air poleward toward the Azores, and high-PV air equatorward into the subtropics. The advection of low-PV air over the Azores leads to a dramatic increase in geopotential heights (not shown). Concurrently, we observe an intensification of the PV gradient over the northern part of the basin, extending northeastward toward the British Isles. Consistent with the sharp PV gradient, the jet strengthens and tilts poleward, in a manner characteristic of the positive phase of the NAO.

Reflective and nonreflective events show similar synoptic features prior to breaking. In the days prior to breaking, a zonally oriented wave train propagates over the North American continent along a strong PV gradient. As the wave train propagates into the western North Atlantic, it encounters a weakened PV gradient, permitting the wave train to propagate equatorward toward the subtropics. Upon approaching the weaker westerly background flow in the subtropics, the wave amplifies, tilts, and imposes a strong poleward eddy momentum flux (associated with the strong equatorward wave activity flux) before the PV field becomes highly nonlinear and breaking occurs.

Directly resulting from PWB, low-PV air (of tropospheric origin) is advected anticyclonically poleward toward the Azores, while high-PV air (of stratospheric origin) is advected equatorward into the subtropics. Unique to PWB over the Atlantic, anomalously high PV is concurrently observed near the Icelandic low. This allows for the formation of a meridionally oriented tripole (e.g., in PV and streamfunction), positioned over the subtropical, midlatitude, and subpolar regions, of which the northern two nodes characterize the NAO (Fig. 2). Although the subtropical location of wave

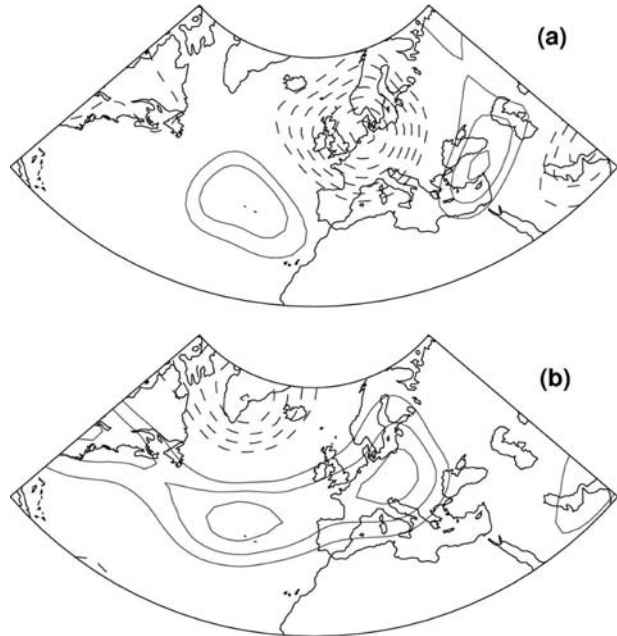


FIG. 3. Anomalous 300-hPa streamfunction 5 days after PWB for (a) reflective and (b) nonreflective PWB. Contours exceeding $2 \times 10^6 \text{ m}^2 \text{ s}^{-2}$ are shown every $1 \times 10^6 \text{ m}^2 \text{ s}^{-2}$.

breaking does not directly impact the subpolar node of the NAO, the anomalous eddy momentum flux associated with PWB appears to excite this mode of variability. This point will be addressed in greater detail in section 3b.

a. Differences between reflective and nonreflective events following breaking

Even though the upper-tropospheric flow fields evolve similarly prior to breaking, profound differences arise between reflective and nonreflective events following breaking. For reflective events (25% of all PWB), anomalies over the North Atlantic rapidly evolve into a poleward arching wave pattern over the Eurasian continent in the ensuing days. While hints of this wave train are evident 2 days following the break, a clear signal is seen extending well over Europe and into the Middle East 5 days after the break, as is evident in the composite 300-hPa streamfunction anomaly (Fig. 3a). The signal of reflection is characterized by a wave train with negatively tilted phase lines (NW–SE) that propagates away from the breaking region.

Conversely, nonreflective events do not show evidence of wave propagation outside of the North Atlantic Basin. Figure 3b shows the composite 300-hPa streamfunction anomaly 5 days after the break. In the days following breaking, the subpolar and midlatitude anomalies amplify and remain stationary as a meridi-

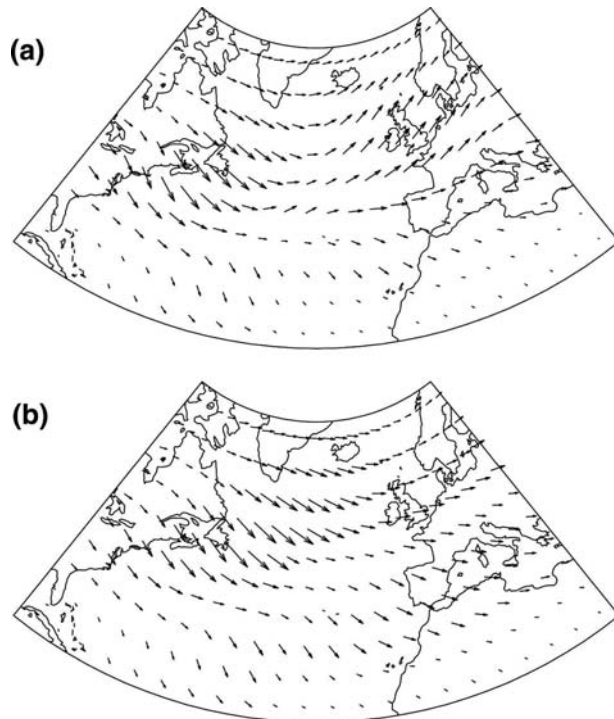


FIG. 4. Composite stationary wave activity flux at 300 hPa for (a) reflective and (b) nonreflective PWB events. Largest vector shown is of magnitude $50 \text{ m}^2 \text{ s}^{-2}$.

onal dipole, akin to the NAO, while the subtropical anomaly dissipates. Thus, nonreflective PWB appears to project prominently onto the positive NAO.

A composite of the quasi-stationary wave activity flux for the reflective PWB cases is shown in Fig. 4a. Reflection is manifested by noting the redirection of the wave activity flux over the basin. Over the western basin it is directed to the southeast, whereas over the eastern basin, north of the wave-breaking region, the wave activity flux is directed to the northeast. The orientation of the wave activity flux over the eastern North Atlantic and western Europe indicates an export of wave activity out of the Atlantic basin, and is consistent with wave propagation over the continent as seen in Fig. 3a. This is suggestive of a wave source region near the Azores associated with reflection (or reradiation) from the wave-breaking region, and a wave sink farther poleward. This picture suggests that reflective events invoke a reversal in the winter mean picture of wave source/sink regions over the subpolar and subtropical North Atlantic (e.g., Fig. 4 in Plumb 1985).

For the composite of nonreflective cases of PWB, the wave activity flux is directed equatorward over the North Atlantic and western Europe (Fig. 4b). A noted region of wave activity flux divergence (wave source)

exists at subpolar latitudes, while wave absorption (flux convergence) is observed over the Azores and western Europe. In stark contrast to the reflective events, the quasi-stationary wave activity flux over the North Atlantic for nonreflective events amplifies the climatological wave source/sink features over the North Atlantic, through an enhanced and prolonged poleward eddy momentum flux. These results appear consistent with anomalies in Rossby wave sources and sinks associated with the developing positive phase of the intraseasonal Northern Hemisphere annular mode (NAM; McDaniel and Black 2005). In addition, the prolonged strong equatorward wave activity flux (a necessary precursor to PWB) encourages further wave breaking events over the Atlantic.

b. A closer look at differences in the eddy momentum flux following breaking

We examined upper-tropospheric eddy momentum flux divergence fields to assess variations in wave-induced momentum transport between reflective and nonreflective cases of breaking. The relationship between eddies and annular modes has been investigated extensively in the literature (e.g., Yu and Hartmann 1993; Limpasuvan et al. 2000; Vallis et al. 2004). It is known that eddy-driven jets are forced by the eddy momentum flux. Vacillations in eddy stirring can alter the strength and latitude of the jet, thus resulting in the well-known dipole feature characteristic of annular modes. Vallis et al. (2004) showed in an idealized model that the momentum flux alone can drive intraseasonal variations in annular modes. Here, we examine the barotropic wave forcing by vertically integrating the eddy momentum flux between 500 and 100 hPa. We isolate the time scales of wave driving into high- and low-frequency components as follows:

$$G_H = \int_{100}^{500} u'_H v'_H dp, \quad (1)$$

$$G_L = \int_{100}^{500} u'_L v'_L dp, \quad (2)$$

where subscripts H and L refer to transients with time scales less than 10 days and greater than 10 days (but less than the seasonal cycle), respectively. We calculate deviations from the zonal mean and average over 0° – 70°W .

Figure 5 shows the composite time evolution of the latitudinal convergence of eddy momentum flux for high-pass- (panels a and c) and low-pass- (panels b and d) filtered transients over the North Atlantic sector, associated with reflective (panels a and b) and nonre-

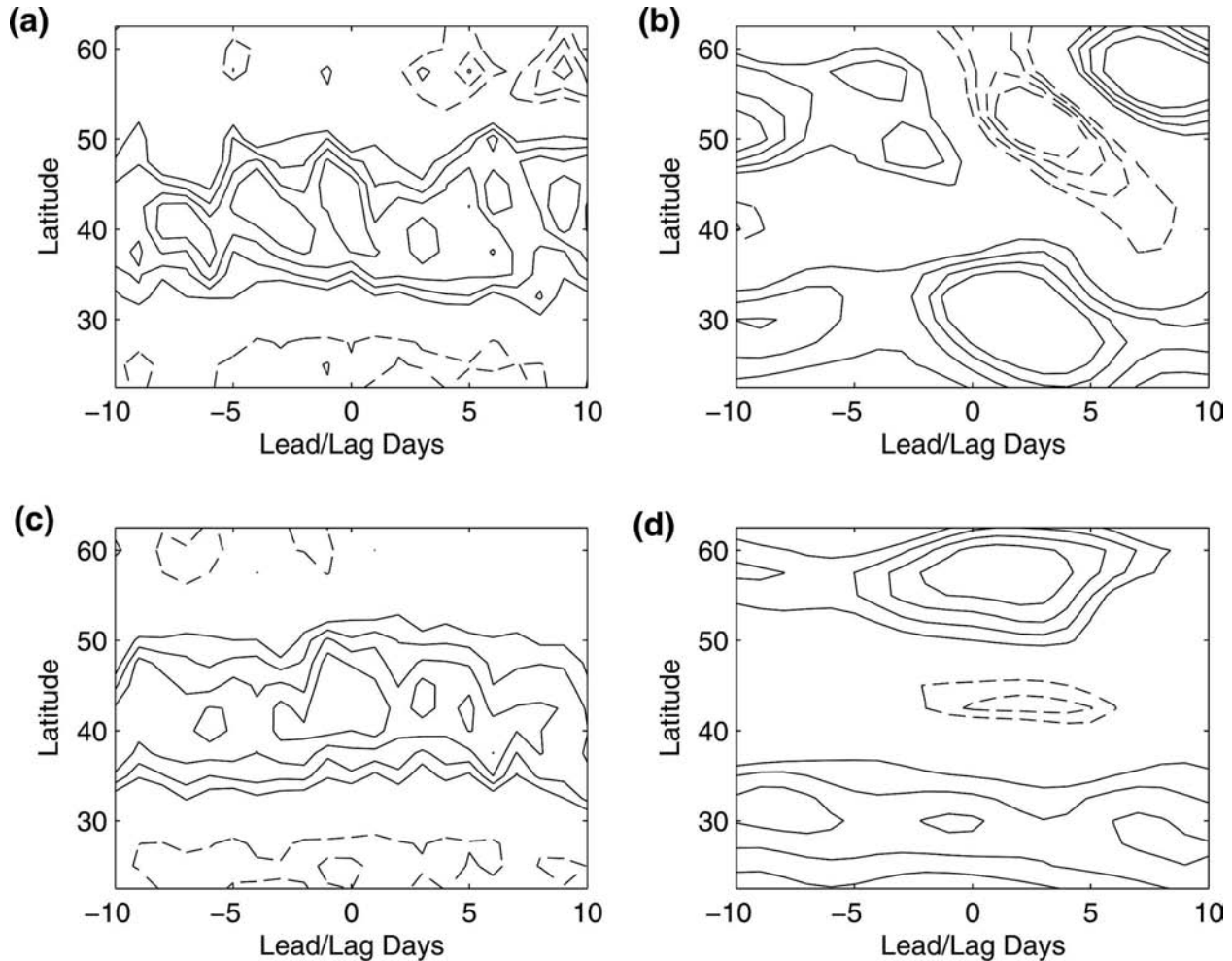


FIG. 5. Composite time evolution of eddy momentum flux convergence at 300 hPa, averaged over 0° – 70° W, attributed to [left, (a), (c)] high-frequency transients and [right, (b), (d)] low-frequency transients. Composites of reflective PWB are shown on top [(a), (b)], while composites for nonreflective events are shown at the bottom [(c), (d)]. Contours for convergence (divergence) are shown by solid (dashed) contours exceeding $8 \times 10^{-6} \text{ m s}^{-2}$, with a contour interval of $4 \times 10^{-6} \text{ m s}^{-2}$.

flective (panels c and d) cases of breaking. As mentioned previously, a large poleward eddy momentum flux is noted prior to breaking. This corresponds to a wave train with positively tilted (NE–SW) phase lines observed during anticyclonic PWB, whereby wave activity is directed equatorward and westerly momentum is directed poleward. The high-pass-filtered transient eddy momentum flux shows a well-defined band of convergence near 45° N that increases near the day of the breaking event. This is consistent with the notion that the high-frequency transients are important in driving the climatological eddy-driven jet over the Atlantic. Differences between reflective and nonreflective cases are not significant.

The low-frequency eddy momentum flux is more revealing. Two latitudinal bands of eddy momentum convergence are noted near 30° and 55° N. Large differ-

ences between reflective and nonreflective cases are apparent following the break. For reflective cases (Fig. 5b), there is a large increase in eddy momentum convergence near the subtropical jet. At the same time, a well-defined region of eddy momentum flux divergence develops near 55° N. Herein lies the signal of the reflection, as the reversal of the meridional wave activity flux results in anomalous eddy momentum flux convergence equatorward of the jet and anomalous eddy momentum flux divergence poleward of the jet.

In contrast, nonreflective cases (Fig. 5d) show a prolonged piling up of zonal momentum near 60° N peaking about 3 days after the break. This analysis is consistent with the observed acceleration of the zonal flow at this latitude due to pronounced low-frequency wave driving.

Although the signal of PWB and nonlinear reflection

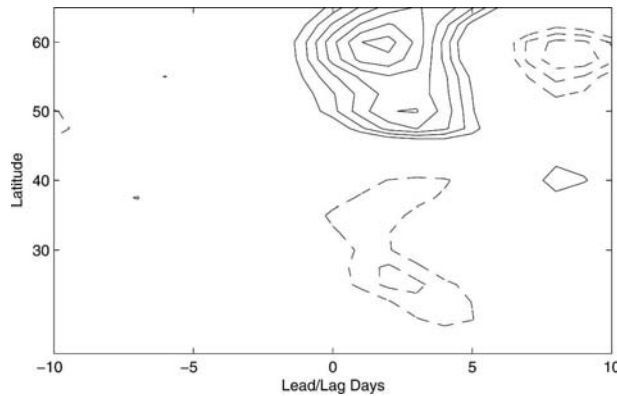


FIG. 6. Composite difference between nonreflective and reflective cases of PWB in the time evolution of the zonal-mean zonal wind tendency averaged between 500 and 100 hPa. Contours are shown every $0.1 \text{ m s}^{-1} \text{ day}^{-1}$ exceeding $0.3 \text{ m s}^{-1} \text{ day}^{-1}$.

is apparent only over the Atlantic sector, breaking contributes notably to the anomalous wave driving of the zonal-mean flow. Here we consider a simplified version of the quasigeostrophic, zonal-mean, zonal-momentum equation:

$$\frac{\partial[\bar{u}]}{\partial t} = \frac{\partial[\overline{u'v'}]}{\partial y} + f_0[v_a], \quad (3)$$

where friction is neglected. Dynamical fields are integrated vertically from 500 to 100 hPa. The overbar indicates zonal average, the prime deviation from zonal average, and the square brackets indicate vertical integration. Results for the zonally averaged case are very similar to those presented in Fig. 5, although shifted slightly equatorward. Figure 6 shows the time evolution of the difference in vertically averaged zonal-mean, zonal wind tendencies between nonreflective and reflective PWB events. Compared to reflective events, nonreflective events show a $0.8 \text{ m s}^{-1} \text{ day}^{-1}$ acceleration of the zonal-mean zonal wind between 55° and 60°N in the days following breaking. A weaker zonal-mean zonal wind tendency of opposite sign is noted near 30°N . Dividing the eddy momentum flux into high- and low-pass contributions, as we did for the regional eddy momentum flux, reveals that the differences between zonal-mean wave driving are primarily a response of the low-pass-filtered eddies. The picture presented here indicates that the upshot of North Atlantic PWB may influence the NAM (or Arctic Oscillation), thus having a hemispheric influence.

4. Connection to the intraseasonal and interannual NAO

As an objective means of documenting the opposing impacts observed between reflective and nonreflective PWB, we compute a time series that approximates the

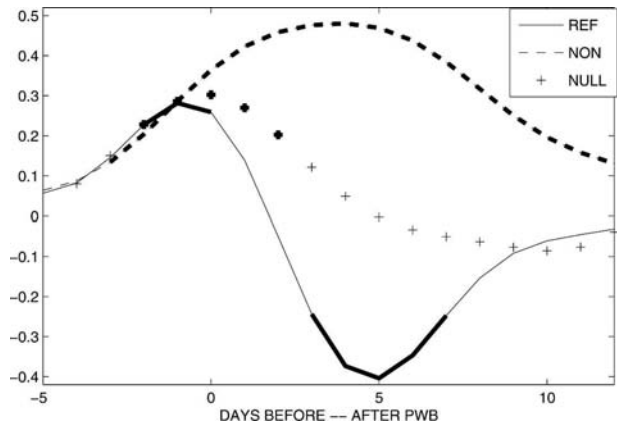


FIG. 7. Composite lead-lag NAOI for reflective (solid) and nonreflective (dashed) PWB events. The composite NAOI for the corresponding null case is indicated by the plus sign (+). Boldface print indicates statistical significance exceeding the 95% confidence interval.

NAO index (NAOI). The NAOI is computed from the leading time series (i.e., principal components) of the first rotated EOF of daily 300-hPa geopotential heights, following Feldstein (2000). A 6-day low-pass filter is then applied to this time series to filter out subsynoptic-scale features. Figure 7 shows the composite lead-lag NAOI with respect to the day of the break for reflective and nonreflective cases of PWB. In both cases the NAOI tends toward a positive state leading up to the day of the break. For reflective cases, the NAOI peaks just prior to breaking, after which it rapidly decreases and reverses sign. Statistically significant anomalies (at the 95% level) are noted 3–7 days after reflective PWB. Conversely, for nonreflective events, the NAOI continues its positive tendency, before peaking 4 days after the break. After reaching its maximum amplitude, the NAOI remains positive (statistically significant) for more than 10 days after the break. Figure 7 succinctly characterizes the prominent differences in the NAO life cycle between reflective and nonreflective cases of PWB, as discussed in section 3. The relationship between reflective–nonreflective PWB and the NAOI holds throughout the 45-yr record independent of the winter-mean phase of the NAO.

To establish that PWB is instrumental in perturbing the intraseasonal NAO, we examine a null case. The null case identifies pentads of anomalous equatorward wave activity flux (F_y) over the NW Atlantic sector (35° – 55°N , 35° – 75°W) for which PWB does not take place. Anomalous equatorward F_y over the aforementioned sector is observed prior to breaking events over the Atlantic basin, and may be considered a precursor to breaking. The null case captures large-amplitude equatorward-propagating linear Rossby waves that do

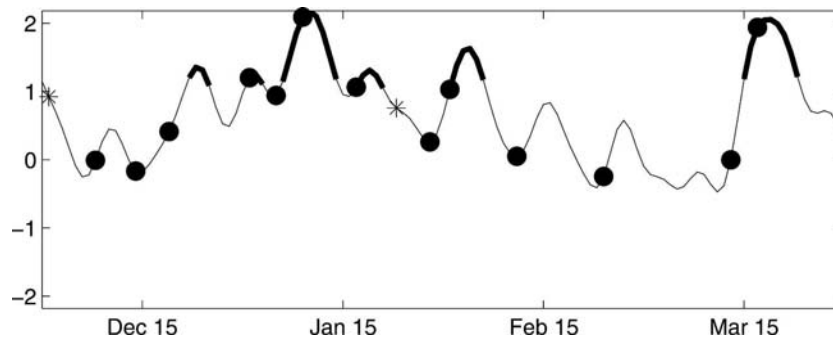


FIG. 8. Daily NAOI for DJFM 1992–93. Days where reflective and nonreflective PWB are observed are indicated by asterisks (*) and filled circles (●), respectively. Periods classified by a persistent positive NAO (PPN) are denoted by a boldface curve.

not break over the Atlantic. They are therefore dynamically distinct from the identified cases of PWB.

Pentad mean wave activity flux is calculated for the complete 45-yr December–March (DJFM) period. Pentads whereby F_y exceeds the average equatorward wave activity flux preceding PWB events ($\overline{F_y(\text{PWB})}$) are retained. We then filter out pentads for which PWB has been identified either during or in the ensuing pentad. Although nearly 350 pentads were identified for which $F_y \geq \overline{F_y(\text{PWB})}$, a vast majority (72%) of these pentads coincide with or are directly followed by a PWB event.

The composite NAOI for the null case (100 events total) is overlaid in Fig. 7 by the plus signs.² Similar to the increase in NAOI observed prior to PWB, we observe an increase in the NAOI during the pentad of anomalous F_y for these nonbreaking events. However, the anomaly quickly subsides thereafter, resulting in a near-neutral NAOI. The null case adds further credence to the dynamical importance of PWB in the development of the intraseasonal NAO. While anomalies in F_y appear to accompany the positive phase of the NAO, their impact appears to be short lived in the absence of PWB, or when nonlinear reflection takes place following PWB. Thus, nonreflective wave breaking appears to serve as an important mechanism in forcing the positive phase of the NAO by effectively trapping wave activity within the North Atlantic basin thus allowing for continued anomalous poleward eddy momentum flux.

By using composites in our analysis, we acknowledge that strong perturbations are likely canceled by weaker perturbations. We address this point by examining the impact PWB has on the genesis of a persistent positive NAO (PPN). Persistent events are defined when the NAOI exceeds one standard deviation (σ) for at least 3

consecutive days, similar to the methodology put forth in Feldstein (2003). For each PWB event we examine the NAOI for the 6 days following the break. A PPN is diagnosed when there are at least 3 consecutive days where the $\text{NAOI} \geq \sigma$ over these 6 days. PPNs were found following nearly 36% of the nonreflective events (156 cases), and less than 12% of the reflective events (16 cases). For comparison, we found PPNs to occur less than 11% of the time for periods that are separated by at least 4 days from a PWB event. Thus, the occurrence of a PPN following a nonreflective PWB event is over three times more likely than the occurrence following a reflective PWB or non-wave-breaking event.

A search for PPNs over the entire DJFM time series for the 45 winters is performed. This results in the identification of 124 distinct PPNs, comprising over 1100 total days. We then filter out cases of PPNs for which wave breaking is observed within 3 days prior to the initiation of a PPN. By excluding events that were preceded by PWB, only 44 events remain. This means that nearly 65% of all PPNs are preceded (and/or possibly forced) by PWB.

Figure 8 shows the daily NAOI for the winter of 1992/1993. While the winter-mean NAOI was anomalously positive over the course of this winter, one can easily detect a series of quasi-biweekly oscillations in the daily NAOI with six separate PPNs. Superposed are dates of observed reflective (marked with an asterisk, *) and nonreflective (marked with a filled circle, ●) PWB events. This winter was characterized by an unusually high number of nonreflective PWB events. In agreement with the above-mentioned connection between PWB and PPN, we note that prior to the onset of large positive phases of the NAO (i.e., PPN events denoted by the bold curve) there tends to be a nonreflective PWB event. Furthermore, 10 of the 13 nonreflective events show an upward trend in the NAOI in the days following their occurrence. However, not all non-

² The time frame is shifted such that the pentad with anomalous F_y occupies days -5 to -1 .

reflective events have this effect, as 2 of the 13 nonreflective events are followed by a negative tendency in the NAOI, and one event has a neutral tendency.

We find a strong interannual correlation between the winter-mean NAOI and the number of PWB events during DJFM ($r = 0.586$). Changes in the basic state associated with the positive phase of the NAO lead to a stronger equatorward wave activity flux (Limpasuvan and Hartmann 1999) and a weaker westerly flow over the central and eastern Atlantic near 30°N , both of which act to precondition the subtropical Atlantic to PWB. As suggested by Abatzoglou and Magnusdottir (2006), the increased separation of the eddy-driven and subtropical jets and the weakening of the subtropical PV gradient during the positive phase of the NAO correspond to a leakier waveguide across the Atlantic and an increase in PWB frequency.

To summarize, the outcome of PWB over the North Atlantic in winter in terms of whether the events are reflective or nonreflective influences the phase of the intraseasonal NAO. At the same time the existing phase of the winter-mean NAO largely determines the flow fields for wave propagation (e.g., being more conducive to wave breaking during NAO positive conditions). The statistically significant relation shown in Fig. 7 suggests that the reflective/absorptive behavior of wave-breaking events contributes to the intraseasonal NAO. In addition to permitting the maturation of the positive phase of the NAO, the flow field following nonreflective PWB further predisposes upstream wave trains to propagate equatorward over the Atlantic and break. This is consistent with our finding that wave-breaking events appear episodic in nature such that they tend to be clustered in time (e.g., Fig. 8). It is envisioned that feedback between repetitive nonreflective PWB and the flow field may be partially responsible in composing, or maintaining, the winter-mean NAO.

5. Concluding remarks

Upon analyzing daily fields of PV on several isentropic surfaces in the upper troposphere/lower stratosphere over the course of 45 winters, we identified 576 cases of anticyclonic planetary wave breaking over the subtropical North Atlantic. Of those, 143 PWB events resulted in nonlinear reflection. For both reflective and nonreflective events, we note that the positive phase of the NAO begins to develop as a wave train propagates equatorward over the Atlantic near the jet exit just prior to breaking. Significant wave driving ensues as the wave train breaks in the subtropics and a meridional PV tripole (Fig. 2) forms over the basin. While the

southernmost node of the tripole quickly dissipates through diabatic processes, the two northerly nodes remain strong as they overlap with the NAO, the preferred mode of low-frequency variability over the North Atlantic in winter.

Significant differences in the NAO life cycle arise upon examining composites of reflective and nonreflective cases of PWB. Cases for which nonlinear reflection is identified show evidence of wave propagation poleward and downstream of the wave-breaking region, over the Eurasian continent, and out of the North Atlantic Basin. For nonreflective cases, wave activity piles up over the North Atlantic basin almost as if a wave cavity is formed. This results in an amplification of the NAO-like meridional dipole.

The anomalous poleward eddy momentum flux associated with the PWB event is instrumental in the development of the intraseasonal NAO. Nonlinear reflection results in a reversal in the eddy momentum flux over the North Atlantic, moving the eddy-driven jet southward and reversing the polarity of the NAO. Conversely, nonreflective events represent the more typical case whereby wave breaking leads to the continued forcing of the positive NAO. In terms of simple eddy momentum flux arguments, reflective events reverse the poleward eddy momentum flux leading to the demise of the positive NAO, while nonreflective events exacerbate the anomalous poleward eddy momentum flux leading to the amplification of the positive NAO.

The explicit mechanisms responsible for the outcome of wave breaking are not immediately apparent from our analysis. Daily fields of PV show that many nonreflective events do not break rapidly (within 1 day) and instead meet wave-breaking criteria in the days following the initial diagnosis. As suggested by Abatzoglou and Magnusdottir (2006), prolonged breaking allows dissipative processes to act over an extended time period and over a broadened wave-breaking region, ultimately resulting in the absorption of wave activity in the subtropics. In addition, for reflective events there exists a region of stronger zonal flow and a stronger PV gradient just northeast of the breaking region. A substantial PV gradient downstream of the breaking region provides a duct for wave activity to escape out of the subtropics and for the reflected wave train to propagate into midlatitudes. In the presence of weaker downstream flow, as seen during nonreflective events, the support for linear wave propagation out of the breaking region is suppressed, resulting in prolonged wave breaking and absorption of the wave train in the subtropics.

The close correspondence between PWB and the positive phase of the intraseasonal NAO is rather strik-

ing. Not only do we observe the majority of PPNs to directly follow breaking events, but also there exists a strong interannual correlation between the winter-mean NAOI and the number of PWB events. Changes in the flow field associated with the positive phase of the NAO precondition the subtropical Atlantic for breaking. While the flow field over the North Atlantic is crucial in allowing wave breaking, the result of PWB, being reflective or nonreflective, appears to feed back onto the flow field. We suggest a possible feedback mechanism between nonreflective PWB and the intraseasonal NAO whose integrative effect may extend the influence of PWB on the NAO to seasonal time scales.

Acknowledgments. We thank Steven Feldstein and two other reviewers for comments and suggestions that improved the manuscript. This work is supported by NSF Grant ATM-0301800 and NOAA Grant NA06OAR4310149.

REFERENCES

- Abatzoglou, J. T., and G. Magnusdottir, 2004: Nonlinear planetary wave reflection in the troposphere. *Geophys. Res. Lett.*, **31**, L09101, doi:10.1029/2004GL019495.
- , and —, 2006: Planetary wave breaking and nonlinear reflection: Seasonal cycle and interannual variability. *J. Climate*, **19**, 6139–6152.
- Benedict, J., S. Lee, and S. B. Feldstein, 2004: Synoptic view of the North Atlantic Oscillation. *J. Atmos. Sci.*, **61**, 121–144.
- Brunet, G., and P. H. Haynes, 1996: Low-latitude reflection of Rossby wave trains. *J. Atmos. Sci.*, **53**, 482–496.
- Feldstein, S. B., 2000: The timescale, power spectra, and climate noise properties of teleconnection patterns. *J. Climate*, **13**, 4430–4440.
- , 2003: The dynamics of NAO teleconnection pattern growth and decay. *Quart. J. Roy. Meteor. Soc.*, **129**, 901–924.
- Holton, J. R., P. H. Haynes, M. E. McIntyre, A. R. Douglass, R. B. Rood, and L. Pfister, 1995: Stratosphere–troposphere exchange. *Rev. Geophys.*, **33**, 403–439.
- Kiladis, G. N., 1998: Observations of Rossby waves linked to convection over the eastern tropical Pacific. *J. Atmos. Sci.*, **55**, 321–339.
- Limpasuvan, V., and D. Hartmann, 1999: Eddies and the annular modes of climate variability. *Geophys. Res. Lett.*, **26**, 3133–3136.
- , D. Thompson, and D. Hartmann, 2000: Wave-maintained annular modes of climate variability. *J. Climate*, **13**, 4414–4429.
- Magnusdottir, G., and P. H. Haynes, 1999: Reflection of planetary waves in three-dimensional tropospheric flows. *J. Atmos. Sci.*, **56**, 652–670.
- , and C. C. Walker, 2000: On the effects of the Hadley circulation and westerly equatorial flow on planetary-wave reflection. *Quart. J. Roy. Meteor. Soc.*, **126**, 2725–2745.
- McDaniel, B. A., and R. X. Black, 2005: Intraseasonal dynamical evolution of the northern annular mode. *J. Climate*, **18**, 3820–3839.
- McIntyre, M. E., and T. N. Palmer, 1983: Breaking planetary waves in the stratosphere. *Nature*, **305**, 593–600.
- Plumb, A. R., 1985: On the three-dimensional propagation of stationary waves. *J. Atmos. Sci.*, **42**, 217–229.
- Vallis, G. K., E. P. Gerber, P. J. Kushner, and B. A. Cash, 2004: A mechanism and simple dynamical model of the North Atlantic Oscillation and annular modes. *J. Atmos. Sci.*, **61**, 264–280.
- Walker, C. C., and G. Magnusdottir, 2002: Effect of the Hadley circulation on the reflection of planetary waves in three-dimensional tropospheric flows. *J. Atmos. Sci.*, **59**, 2846–2859.
- , and —, 2003: Nonlinear planetary wave reflection in an atmospheric GCM. *J. Atmos. Sci.*, **60**, 279–286.
- Wallace, J. M., and H.-H. Hsu, 1983: Ultra-long waves and two-dimensional Rossby waves. *J. Atmos. Sci.*, **40**, 2211–2219.
- Yu, J. Y., and D. L. Hartmann, 1993: Zonal flow vacillation and eddy forcing in a simple GCM of the atmosphere. *J. Atmos. Sci.*, **50**, 3244–3259.